Reproducibility is hard

AggreWell™ makes it easy

As more researchers look to 3D spheroid cultures to improve physiological relevance for disease modelling or drug discovery, it is important to ensure that the spheroids are reproducible, no matter the size of your experiment.

Produce uniform 3D spheroids in AggreWell™

Learn More
www.stemcell.com/cancer-spheroids

STEMCELL™ TECHNOLOGIES

Scientists Helping Scientists™ | WWW.STEMCELL.COM

ARTICLE

BIOTECHNOLOGY and BIOENGINEERING

Probing Effects of Pressure Release on Virus Capture During Virus Filtration Using Confocal Microscopy

Shudipto K. Dishari,[1] Adith Venkiteshwaran,[2] Andrew L. Zydney[1]

[1]Department of Chemical Engineering, The Pennsylvania State University, University Park, Pennsylvania 6802; telephone: 814-863-7113; fax: 814-865-7846; e-mail: zydney@engr.psu.edu

[2]Eli Lilly and Company, Indianapolis, Indiana

ABSTRACT: Virus filtration is used to ensure drug safety in the production of biotherapeutics. Several recent studies have shown a dramatic decrease in virus retention as a result of a process disruption, e.g., a transient pressure release. In this work, a novel two-label fluorescence technique was developed to probe virus capture within virus filtration membranes using confocal microscopy. Experiments were performed with Ultipor® DV20, Viresolve® Pro, and Viresolve® NFP membranes using bacteriophage φx174 as a model virus. The filters were challenged with two batches of fluorescently labeled phage: one labeled with red dye (Cy5) and one with green dye (SYBR Gold) to visualize captured phage from before and after the pressure release. The capture patterns seen in the confocal images were a strong function of the underlying membrane morphology and pore structure. The DV20 and Viresolve® NFP showed migration of previously captured phage further into the filter, consistent with the observed loss of virus retention after the pressure release. In contrast, there was no migration of captured virus in the Viresolve® Pro membranes, and these filters were also the only ones to show stable virus retention after a pressure release. The direct visualization of virus capture using the two-label fluorescence technique provides unique insights into the factors controlling the retention characteristics of virus filters with different pore structure.

Biotechnol. Bioeng. 2015;112: 2115–2122.

KEYWORDS: virus filtration; pressure release; bioprocessing; virus clearance; confocal microscopy

Introduction

Viral contamination of biotherapeutics (e.g., recombinant proteins and plasma products) can pose a serious threat to human health. Current FDA regulations require the use of at least two orthogonal viral clearance steps as part of the downstream process for the production of recombinant therapeutics, and essentially all process streams (e.g., media and buffers) are treated to remove any adventitious virus. Virus filtration membranes offer a robust, size exclusion based, removal of virus particles that complements virus inactivation steps. Virus filters are typically designed to provide at least a 4-log (10,000-fold) reduction in virus titer.

Virus filters were originally developed for use in tangential flow filtration with the feed flowing adjacent to the upper skin layer of the asymmetric membrane (DiLeo et al., 1992). Virus retention was a function of device operating conditions, due largely to the effects of concentration polarization (DiLeo et al., 1993). Current operation of virus filters is performed using normal flow filtration due to the simplicity of operation and lower capital cost. These normal flow filters are typically operated with the more open side of the membrane facing the feed allowing protein aggregates and other large foulants to be captured within the macroporous substructure thereby protecting the virus-retentive skin layer (Brough et al., 2002).

Several recent studies have shown that virus retention can deteriorate during normal flow virus filtration (Bolton et al., 2005; Ireland et al., 2004; Lute et al., 2007). In addition, virus retention can be compromised after a process disruption, such as an intermittent release of transmembrane pressure as might occur when the filter is fed from more than one feed tank or when using a buffer flush to recover residual product from the system (Lacasse et al., 2013; Lute, 2014; Woods and Zydney, 2014). For example, Lute (2014) and Lacasse et al. (2013) showed that a pressure release caused a transient 2–3-log reduction in virus retention. Woods and Zydney (2014) obtained extensive data on the effects of a pressure release on retention of φX174 by Ultipor® DV20 membranes. The pressure release caused a transient increase in virus transmission (by more than 1-log), but virus retention then returned to its previous level. Confocal microscopy using a green carboxyfluorescein-labeled phage showed two separate green bands near the entrance of the filter after the pressure release. This behavior was described using a modified version of the internal polarization model developed by Jackson et al. (2014), with some of the

Adith Venkiteshwaran's current address is Harvard Business School, Boston, Massachusetts.
Correspondence to: A.L. Zydney
Contract grant sponsor: Eli Lilly and Company
Received 11 February 2015; Revision received 6 April 2015; Accepted 9 April 2015
Accepted manuscript online 20 April 2015;
Article first published online 12 May 2015 in Wiley Online Library (http://onlinelibrary.wiley.com/doi/10.1002/bit.25614/abstract).
DOI 10.1002/bit.25614

previously captured phage migrating deeper into the filter after the pressure release. However, it was difficult to validate some of the critical assumptions in this model since it was impossible to distinguish between phage that were captured before and after the pressure release.

The objective of the current work was to develop a two fluorescent-dye-based approach to directly visualize captured virus both before and after the pressure release. A series of virus filters were challenged with two batches of φX174, one labeled with the red fluorescent dye Cy5 and the other labeled with the green fluorescent dye SYBR Gold. Confocal images and virus retention data were obtained with three commercial virus filters having very different internal pore structures/morphology: the Ultipor® DV20 from Pall Corporation (Port Washington, NY), the Viresolve® Pro from EMD Millipore (Bedford, MA), and the Viresolve® NFP from EMD Millipore. The results provide unique insights into the mechanisms governing virus capture and retention during virus filtration, including the effects of membrane morphology on virus retention after a process disruption.

Materials and Methods

Membranes

Relatively homogeneous Ultipor® DV20 membranes were purchased as 47 mm disks from Pall Corp. (Port Washington, NY). The DV20 membranes were soaked in water for approximately 1 min; this caused the two layers to separate so that they could be carefully removed using a wide-head tweezers. Highly asymmetric Viresolve® Pro and Viresolve® NFP membranes were provided by EMD Millipore in flat sheet format (single layer). Forty-seven millimeter disks were cut from the sheets and used with the tight skin-side down as per the manufacturer's recommendation.

Bacteriophage

The bacteriophage φX174 (ATCC-13706-B1™) was used as a model virus. This phage is approximately 26 nm in size and it has been used in a number of previous studies of virus filtration membranes (Lute et al., 2007). φX174 were obtained from the American Type Culture Collection (ATCC, Manassas, VA) and propagated in the host *Escherichia coli C* obtained from the *E. coli* Genetic Stock Center at Yale University (New Haven, CT). Luria-Bertani (LB) media was prepared by mixing 10 g/L Bacto™ Tryptone (BD-211705), 5 g/L Bacto Yeast extract (BD-212750), and 10 g/L NaCl in deionized water. The pH was adjusted to 7.5 using NaOH, and the media was then autoclaved and stored in a sterilized cabinet until use. *E. coli* were grown in LB media (35°C) to exponential growth phase, corresponding to an optical density between 0.3 and 0.4. The φX174 was then added to the *E. coli* suspension and incubated at 35°C for 5 h with gentle agitation. The resulting suspension was centrifuged at 3,500 rpm at 4°C at least three to four times to remove the lysate/debris. The supernatant containing the φX174 was decanted and stored at 4°C until use.

Fluorescent Labeling

Fluorescent dyes Cy5 and SYBR Gold were purchased from Sigma–Aldrich (St. Louis, MO) and Life Technologies (Carlsbad, CA), respectively. The Cy5 labeling protocol was developed based on the protein labeling protocol provided by Sigma–Aldrich; the SYBR Gold protocol was adapted from published results for labeling phage P22 (Mosier-Boss et al., 2003) to achieve maximum fluorescence intensity for φX174. The bacteriophage solutions were first concentrated to 4×10^{10} pfu/mL by centrifugation at 3,800 rpm using a spin-concentrator with an Ultracel 100 kDa membrane (EMD Millipore, Billerica, MA) and then buffer exchanged into 0.1 M $NaHCO_3$ (pH 8.5). One milliliter of the phage solution was added to one bottle of Cy5 (approximately 0.2–0.3 mg) and allowed to react for 1 h, with 1 min of vortexing every 10 min. The labeled phage were thoroughly washed with at least 100 diavolumes of 0.1 M $NaHCO_3$ buffer (around 15 wash cycles) using the spin-concentrator to remove free (unreacted) dye. The labeled phage were stored at 4°C and diluted before use. Labeling with SYBR Gold was done as follows: 1.15 mL of a 3×10^9 pfu/mL suspension of φX174 was diluted with 4.84 mL of 1X TAE buffer (MediaTech, Inc., Manassas, VA) and mixed with 5.75 μL of SYBR Gold (10^4 X) dissolved in DMSO. The solution was allowed to react at 4°C for 3 days with gentle mixing. Residual free dye was removed using two or three desalting columns (Econo-Pac 10DG desalting column, 732-2010, BioRad, Hercules, CA). Collected fractions were analyzed using dynamic light scattering, with any fractions containing large particles (>50 nm) discarded. Other fractions were simply pooled.

Virus Filtration

Constant pressure filtration experiments were performed with the virus filters placed shiny-side down, i.e., in the orientation recommended by the manufacturer, in a 47 mm stainless steel filter holder (EMD Millipore Corp.). The phage suspension was ultrasonicated for 45 min, pre-filtered through a 0.2 μm pore size membrane, and then added to a 1 L feed reservoir connected to the filter holder by plastic tubing. The reservoir was air-pressurized, with the pressure controlled at 30 psig using an Ashcroft pressure regulator. Filtrate samples were collected as 1 mL fractions in centrifuge tubes. For the pressure release experiments, the filter was challenged with approximately 12 mL of unlabeled phage, the pressure was released for about 10 min (no transmembrane pressure), and then the filtration was continued at 30 psig for another 12 mL. Confocal images were obtained by first challenging the membrane with 12 mL of Cy5 labeled phage, replacing the feed reservoir with SYBR Gold labeled phage, and then continuing the filtration for an additional 12 mL.

PFU Assay

Phage concentrations in the feed and permeate were measured using a plaque forming unit (pfu) assay as described in the literature (Woods and Zydney, 2014). Briefly, 100 μL phage samples were mixed with 200 μL of *E. coli* suspension and 900 μL of melted soft agar made by adding 4 g/L Difco Agar (BD-214530) to LB media. The

resulting suspension was poured onto hard agar plates made from 10 g/L of Difco agar in LB media. LB media, soft agar, and hard agar solutions were autoclaved for 40 min and stored in a sterilized cabinet until use. The agar plates were incubated at 35°C for 8 h and the number of plaques counted. Plates were made with different dilutions of the original sample to obtain an easily countable number of plaques (typically between 2 and 50 plaques per plate).

Confocal Laser Scanning Microscopy

Virus filtration membranes were imaged with an Olympus Fluoview™ 1000 confocal laser scanning microscope (Upper Saucon, PA) after being challenged with the fluorescently labeled phage following the procedure originally described by Bakhshayeshi et al. (2011). Membranes were cut into small pieces of about 1.5 cm × 1 cm and mounted on a glass slide. A small drop of 10% glycerol was placed on the membrane, which was then covered with a coverslip and sealed to the glass slide using nail-polish. The Cy5 and SYBR Gold dyes were excited with 488 nm (blue) and 610 nm (red) lasers, respectively, with imaging at 510 and 670 nm. A 100× oil objective lens (Numerical Aperture, $NA = 1.25$) was used with zoom magnification set at 2.0. Optical cross-sectioning was done at 0.3 μm intervals, with images at multiple x-y planes stacked to reconstruct a z-image through the depth of the membrane using the Olympus Fluoview™ software. Since the maximum working distance of the oil objective lens is about 80 μm, the Viresolve® Pro and Viresolve® NFP membranes (thickness of 140 μm) were scanned from both sides (flipping the membrane in the microscope), with the two images combined to generate a scan through the full depth of the membrane.

Results and Discussion

Figure 1 shows results for the phage concentration in collected permeate samples obtained with single layer membranes of the Ultipor® DV20, Viresolve® Pro, and Viresolve® NFP filters. Data were obtained with suspensions of φX174 in a 45 mM carbonate buffer at pH 10 using a phage concentration of 8×10^7 pfu/mL (corresponding to a volume fraction of less than 10^{-15}). The data are plotted as a function of the volumetric throughput, defined as the cumulative filtrate volume divided by the membrane cross-sectional area. The dashed vertical lines show the throughput at

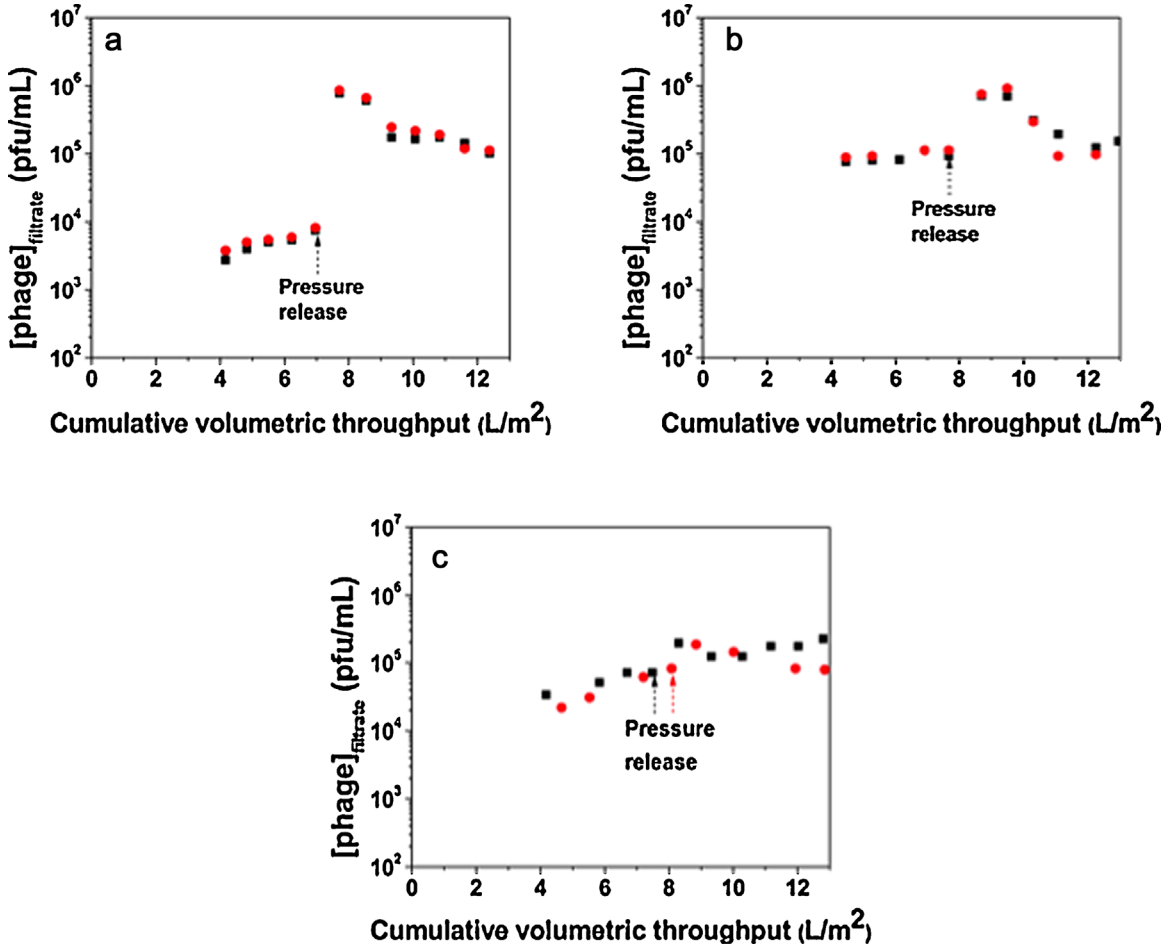

Figure 1. Concentration of bacteriophage in the permeate fractions during filtration of a suspension containing 8×10^7 pfu/mL of φX174 through the (**a**) Ultipor® DV20, (**b**) Viresolve® NFP, and (**c**) Viresolve® Pro filters. The dashed vertical lines show the point where the pressure was released.

which the pressure was released; the pressure was maintained at 210 kPa (30 psi) during the filtration with a 10 min hold at zero pressure after filtration of between 7 and 8 L/m^2. No data are shown for V/A <4 L/m^2 because those samples were diluted by the hold-up volume in the filter holder; this was confirmed using data obtained by filtering the φX174 through a 0.2 μm pore size Supor® 200 membrane that was non-retentive to the phage. The open and closed symbols in the panels show results from repeat experiments performed under identical conditions. The measured phage concentrations were within 0.1 log throughout the virus filtration, both before and after the pressure release, for all three membranes.

The results with the DV20 (Fig. 1a) are similar to those reported previously by Woods and Zydney (2014). There is a slight increase in phage concentration during the first portion of the experiment, with a 2-log (100-fold) increase in phage transmission immediately after the pressure release followed by a more gradual decline. Woods and Zydney (2014) observed a much more rapid decline in phage concentration after the pressure release, with the permeate concentration returning to approximately the value obtained before the pressure release after about 9.5 L/m^2. The filtrate flux during filtration of φX174 through the DV20 membrane (data not shown) remained nearly constant during the initial stage of the filtration at a value of 8.0×10^{-6} m/s (30 L/m^2/h) but increased by approximately 30% immediately after the pressure release and then remained constant. The origin of this increase in flux is unclear; this behavior was not seen by Woods and Zydney (2014) under similar conditions but using a very different lot of membranes. Note that the total volume of phage filtered through the membrane in these experiments would correspond to less than one part in 10^{13} of the membrane volume; thus, phage–phage interactions should be negligible.

The behavior of the Viresolve® NFP (Fig. 1b) was qualitatively similar to that of the DV20, although the phage concentration in the permeate only increased by about 1-log (10-fold) after the pressure release. The filtrate flux for the Viresolve® NFP showed a slight decline throughout the filtration, decreasing from 7.7×10^{-5} m/s (280 L/m^2/h) to 5.4×10^{-5} m/s. The much higher flux for the Viresolve® NFP compared to the DV20 is consistent with the much higher permeability of the highly asymmetric Viresolve membrane.

In contrast to the results obtained with the DV20 and Viresolve® NFP, phage transmission through the Viresolve® Pro was essentially unaffected by the pressure release (Fig. 1c), although there was a slight continuous increase in the phage concentration in the filtrate throughout the experiment. In addition, there was no significant flux decline during filtration of the φX174 through the Viresolve® Pro, with the flux remaining within ± 5% of the initial value (5.8×10^{-5} m/s = 210 L/m^2/h).

Figure 2 shows cross-sectional confocal images of two Ultipor® DV20 membranes, one used to filter approximately 8 L/m^2 of SYBR gold-labeled φX174 (left panel) and one used to filter approximately 8 L/m^2 of Cy5-labeled phage followed by 8 L/m^2 of the SYBR gold-labeled phage after a pressure release for 10 min (right panel). Limited experiments performed with φX174 that had been pre-filtered through a DV50 membrane (with 50 nm pore size) showed nearly identical images, indicating that the capture patterns were not due to the presence of large aggregates in the phage challenge. In both experiments, the phages were captured near the filter inlet, consistent with the slight asymmetry in the pore size of the DV20 membrane (Bakhshayeshi et al., 2011). This upper region was described by Jackson et al. (2014) as the "reservoir zone" within the DV20 membrane. The results obtained after the pressure release experiment were quite different, with the red phage (in the challenge before the pressure release) captured in two distinct bands separated by approximately 5 μm within the depth of the filter. The green phage (in the challenge after the pressure release) are seen primarily as a single band slightly upstream of the red band (closer to the entrance of the filter). The bands in the right panel are much "sharper" than the single band in the left panel; this is likely due to the inherent variability between membrane samples. There was also some variability in images obtained at different locations within a given filter, although the qualitative behavior was very reproducible.

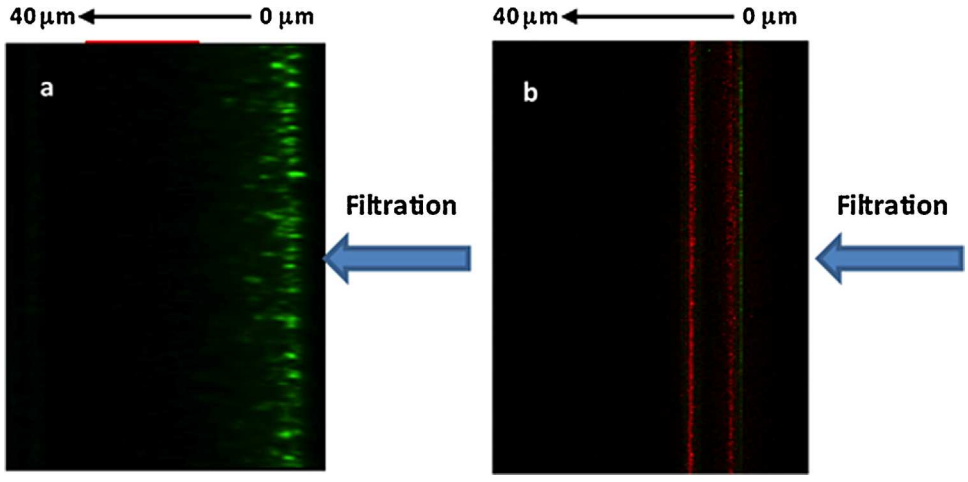

Figure 2. Cross-sectional images of Ultipor® DV20 membranes after filtration of fluorescently labeled φX174 at constant pressure (left) and after a pressure release experiment (right). The Cy5-labeled (red) phage was used in the challenge before the pressure release, with the SYBR gold-labeled (green) phage after pressure release.

Woods and Zydney (2014) saw similar capture profiles for the DV20 membrane after a pressure release experiment, although the images were obtained using only green-labeled phage, making it impossible to distinguish between the phage that were in the challenge before versus after the pressure release. They hypothesized that the captured phage were able to diffuse out of the retentive pores during the pressure release, migrating laterally within the filter and then moving deeper into the filter (with some phage passing all the way into the filtrate) when the pressure was reapplied. This physical picture is in good agreement with the two-label image obtained after the pressure release in Figure 2. In this case, some of the red phage that were captured before the pressure release appear to have moved deeper into the membrane (with some phage remaining in the initial band near the upstream surface of the filter). The green phage, which were filtered after the pressure release, were captured almost entirely in a single layer located just upstream of the top layer of the red phage.

The confocal images obtained with the Viresolve® Pro looked markedly different. The image obtained after the constant pressure filtration (Fig. 3) showed multiple bands within the Viresolve® Pro membrane, including a fairly bright band approximately 25 μm in from the upstream surface of the membrane and then a more diffuse band near the exit of the membrane. The upper band occurred in the microporous support layer of the Viresolve® Pro membrane as seen in the SEM image in Figure 4. This can also be easily seen in the x-y confocal image at a depth of 26 μm where the dark regions (areas without any fluorescence) correspond to the pores. The fluorescence seen in this region was probably not due to the capture of large aggregates of the φX174; images obtained with phage that had first been prefiltered through an Ultipor® DV50 membrane (pore size of approximately 50 nm, which should remove any aggregated phage) looked nearly identical to the image seen in Figure 3 (image not shown). It is possible that the fluorescence in this region of the filter is due to adsorption of phage (or labeled debris) to the membrane surface, although it is unclear why this would occur in a relatively narrow band instead of throughout the microporous support. Additional studies would be needed to determine the nature of the capture in this upper region of the membrane.

The diffuse band of captured phage near the filter exit was located within the graded pore structure of the dense region of the Viresolve® Pro membrane (SEM image in Fig. 4). In contrast to the DV20, which has a relatively uniform pore size throughout the depth of the filter, the Viresolve® Pro is highly asymmetric, with the pore size decreasing throughout the dense layer as one approaches the highly retentive "skin" on the downstream (exit) surface of the filter (the "shiny side"). The phage appear to be captured in a uniform layer distributed across the x-y plane (panel at a depth of 118 μm). Note that individual pores (around 20 nm in size) in this region of the membrane cannot be resolved in the confocal image

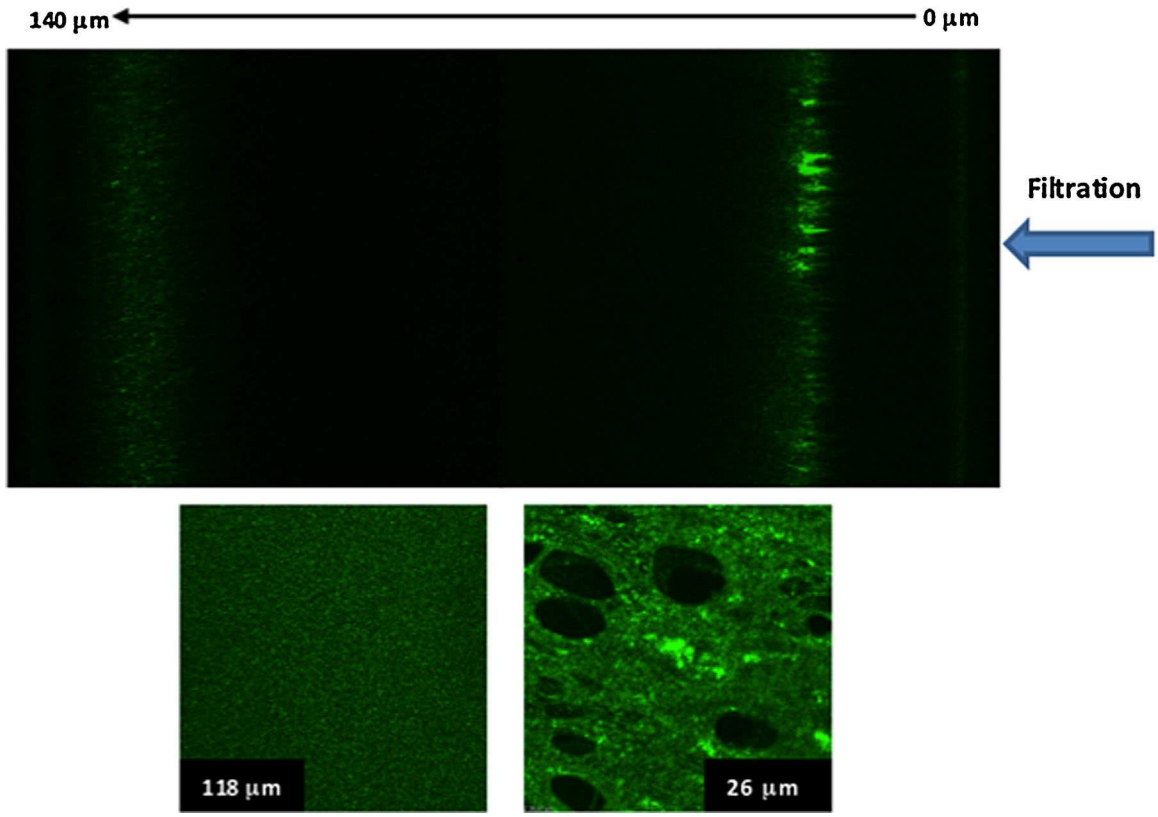

Figure 3. Confocal images of the Viresolve® Pro membrane obtained after filtration of 8 L/m^2 of a 8 × 10^7 pfu/mL suspension of the φX174 labeled with SYBR Gold. Lower images show x-y planes at depths of 26 and 118 μm within the 140 μm membrane.

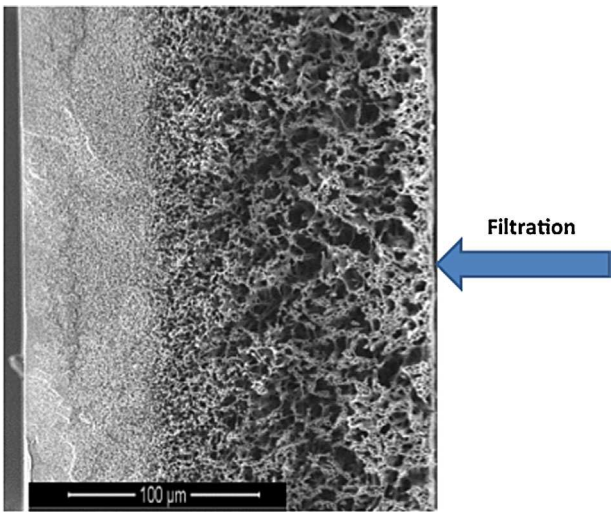

Figure 4. Scanning electron micrograph (SEM) of the cross-section of a Viresolve® Pro membrane (image courtesy of Sal Giglia at EMD Millipore).

since the lateral resolution is limited by the wavelength of light to at best 200 nm. The very diffuse band (in the z-direction) seen in the confocal image likely reflects the pore size distribution within the filter in combination with the stochastic nature of phage capture, with the probability of capture increasing as the pore size narrows through the depth of the filter.

Figure 5 shows the corresponding images obtained after a pressure release experiment in which the Cy5-labeled (red) phage were filtered through the Viresolve® Pro before the pressure release while the SYBR Gold-labeled (green) phage were filtered after the pressure release. Both the red and green phage were seen in multiple bands, with the band near the entrance of the filter showing nearly equal and uniform intensity of both labeled phage. In contrast, the broader band near the exit of the filter began as predominantly red (moving in from the upstream surface of the filter) but became predominantly green as one moved toward the filter exit (seen more clearly in the images of the x-y planes at different depths within the filter). There was no evidence of any migration of the red phage deeper into the filter after the pressure release. Instead, the phage that were captured during the initial portion of the filtration (before the pressure release) seemed to remain at the same location within the filter, while the phage captured after the pressure release were located somewhat deeper within the filter (nearer the filter exit).

The confocal images in Figure 5 suggest that virus capture in the Viresolve® Pro occurs at specific "retentive sites" within the filter,

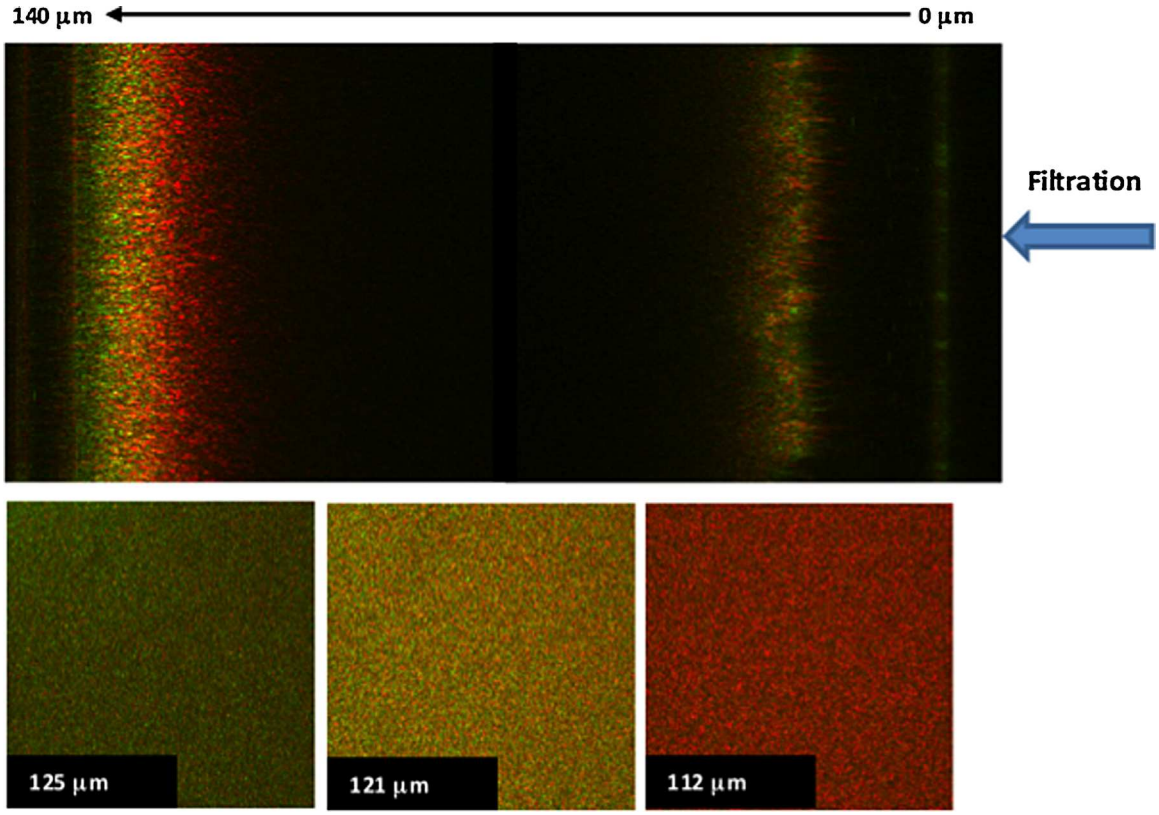

Figure 5. Confocal images of the Viresolve® Pro membrane after filtration of a suspension of fluorescently labeled φX174. Cy5-labeled (red) phage were used in the 8 L/m^2 challenge before the pressure release; SYBR Gold-labeled (green) phage were used in the 8 L/m^2 challenge after the pressure release. Lower images show x-y planes at depths of 112, 121, and 125 µm within the 140 µm membrane (corresponding to band near the filter exit toward the left-side of the top image).

e.g., at regions where the flow passes through pores in which the pore "throat" is smaller than the size of the φX174. As the filtration continues, these retentive sites become filled, with subsequent phage being carried deeper within the filter where they are captured at "retentive sites" located closer to the filter exit. This is clearly seen in the two-label experiments, with the green phage (in the challenge after the pressure release) captured in a diffuse band that lies further into the depth of the filter.

Figures 6 and 7 show corresponding data for the lower half of the Viresolve® NFP membrane; Figure 6 shows results for an experiment using a constant pressure with the SYBR Gold-labeled phage, while Figure 7 shows results for a pressure release experiment involving the filtration of the Cy5 followed by the SYBR Gold-labeled phage. The confocal image in Figure 6 shows two bands deep within the filter within the porous region of the membrane but well above the highly retentive skin layer (at the far left of the image). The origin of this "double band" is unclear, although it may be related to the gradation in pore size within the asymmetric Viresolve® NFP membrane.

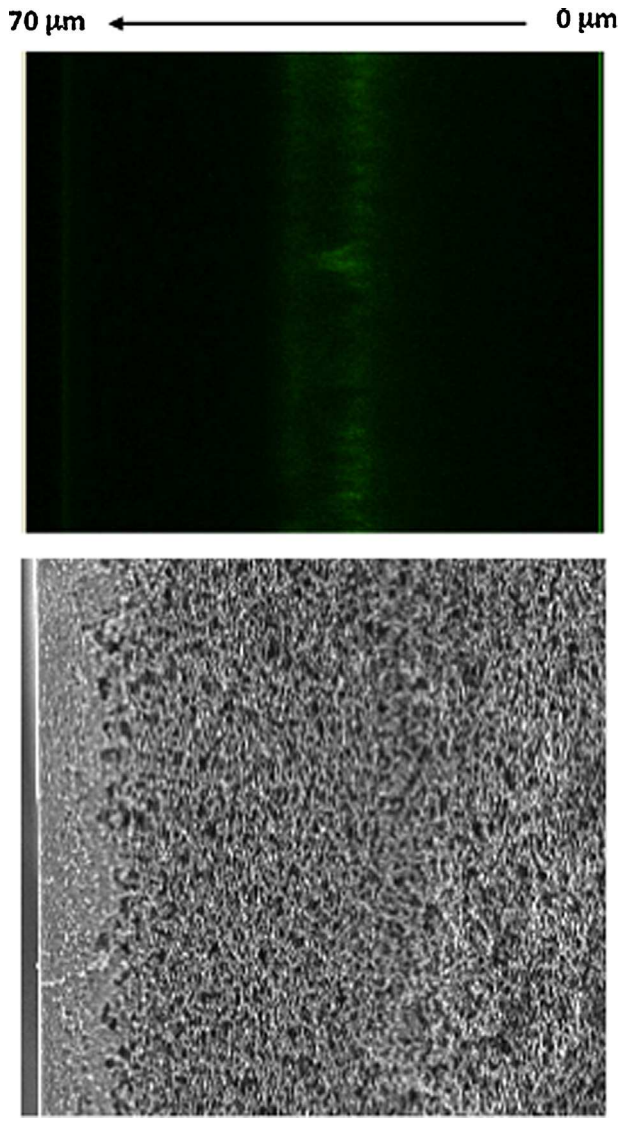

Figure 6. Confocal images of the Viresolve® NFP membrane obtained after filtration of 8 L/m^2 of a 8×10^7 pfu/mL suspension of the φX174 labeled with SYBR Gold. Lower panel shows SEM image of lower half of Viresolve® NFP membrane (image courtesy of Sal Giglia at EMD Millipore).

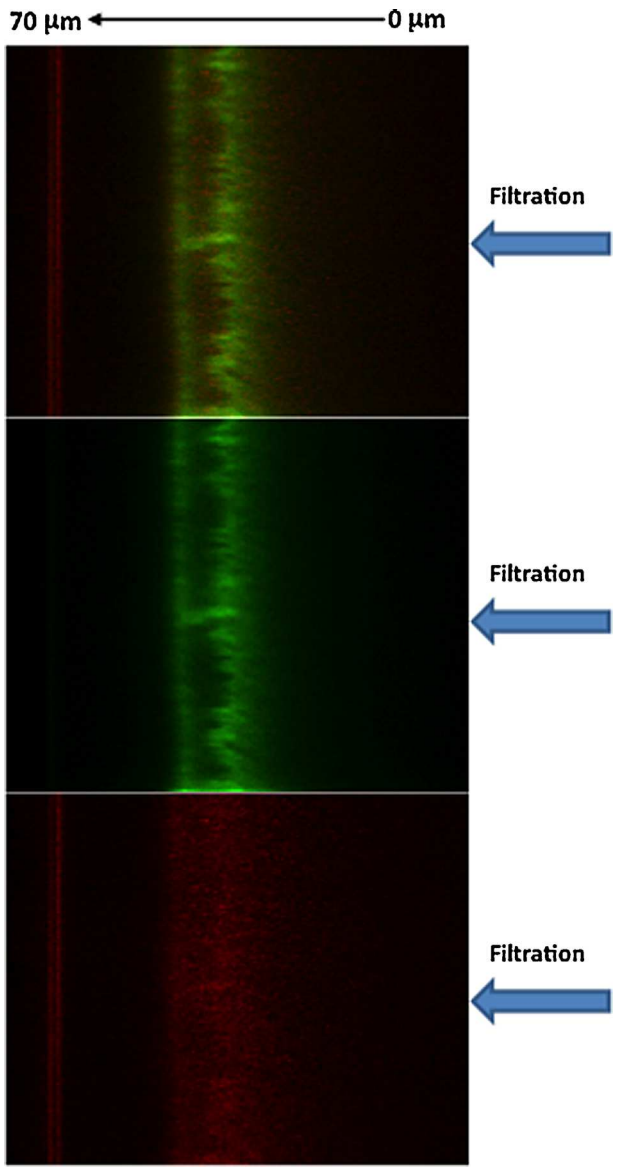

Figure 7. Confocal images of the lower half (near the filter exit) of the Viresolve® NFP membrane after filtration of φX174 in a pressure release experiment. Cy5-labeled (red) phage were used in the 8 L/m^2 challenge before the pressure release; SYBR Gold-labeled (green) phage were used in the 8 L/m^2 challenge after the pressure release. Lower panel shows excitation of Cy5. Middle panel shows SYBR-Gold. Upper panel shows overlay of the images.

Figure 7 shows results for the pressure release experiment. Separate images are shown at emission wavelengths of 510 nm and 670 nm to more clearly visualize the phage that were captured before (red) and after (green) the pressure release; the upper panel shows an overlay of these images. Note that the overlay is done

automatically within the Olympus Fluoview™ software (without any manual alignment). Most of the Cy5-labeled phage were captured in a diffuse band within the tighter pore region of the membrane but located closer to the feed-side (see SEM image in lower panel of Fig. 6), although there was also a very narrow band at the membrane exit (far left of image) that may represent phage that were captured within the membrane before the pressure release and then migrated deeper within the membrane during the second half of the filtration experiment (after the pressure release). The SYBR Gold-labeled (green) phage were almost completely absent from the lower band near the exit of the membrane, consistent with the presence of these phage only in the challenge after the pressure release.

Conclusions

Virus filtration is a critical component of the overall virus clearance strategy for the production of recombinant protein therapeutics. Recent results showing a decline in virus retention in response to a process disruption have generated questions about the mechanism of virus capture during virus filtration and concerns about whether retention could be compromised under some conditions. In this work, a novel two fluorescent-dye technique was developed to directly visualize virus captured within different virus filters both before and after a pressure release, providing unique insights into the virus capture phenomenon that compliment data for virus transmission.

Phage transmission through the Ultipor® DV20 and Viresolve® NFP membranes increased after a short pressure release, by approximately 2 and 1 logs (100- and 10-fold), respectively. Virus capture in the DV20 membrane after a pressure release experiment showed two distinct bands for the phage captured before the pressure release, while the phage captured after the pressure release were located almost entirely in a narrow band near the entrance of the filter. Virus capture in the Viresolve® NFP was more complicated, with multiple capture bands near both the entrance and exit of the filter, but the images obtained after a pressure release also show the migration of previously captured phage deeper within the filter—this migration was only visible because of the use of the two-label fluorescent technique developed in this work. These results suggest that previously captured virus within the DV20 and Viresolve® NFP membranes are able to diffuse out of the pores (capture sites) when the filtration pressure is removed, with the released phage either recaptured deeper within the filter or transmitted through the membrane when the filtration is continued. This behavior is qualitatively consistent with predictions of the internal polarization model proposed by Woods and Zydney (2014) and Jackson et al. (2014), although the more complex capture pattern seen with the Viresolve® NFP would likely require a much more sophisticated mathematical description.

Even though the Viresolve® Pro is also highly asymmetric (like the Viresolve® NFP), it showed a very different virus capture and transmission behavior. Measurements of phage transmission showed no measurable difference before/after a pressure release, consistent with the absence of any migration of previously captured phage in the two-label confocal images. Instead, the phage that were filtered after the pressure release appear to be captured deeper within the membrane, migrating past the sites that were filled with previously captured phage. This very different behavior is likely related to the different morphology of the pores in the Viresolve® Pro, which minimize (or even eliminate) the back-diffusion of previously captured phage. Additional studies will be needed to identify the mechanisms governing the back-diffusion phenomenon in virus filters and its relationship to the underlying pore structure. The results presented in this study clearly demonstrate that confocal microscopy using a two-label fluorescence technique provides unique insights into virus retention that could not be obtained using previously developed methods, potentially facilitating the development of more effective virus filtration membranes/processes for purification of high-value therapeutic products.

The authors acknowledge financial support from the Lilly Research Award Program (LRAP) from Eli Lilly and Company. The authors also thank EMD Millipore for providing the single layer Viresolve® Pro and Viresolve® NFP membranes and Professor Wayne Curtis and his research group for assistance with the bacteriophage propagation and pfu assay.

References

Bakhshayeshi M,Jackson N, Kuriyel R, Mehta A, van Reis R, Zydney AL. 2011. Use of confocal scanning laser microscopy to study virus retention during virus filtration. J Membrane Sci 379:260–267.

Bolton G, Cabatingan M, Rubino M, Lute S, Brorson K, Bailey M. 2005. Normal-flow virus filtration: Detection and assessment of the endpoint in bioprocessing. Biotechnol Appl Biochem 42:133–142.

Brough H, Antoniou C, Carter J, Jakubik J, Xu Y, Lutz H. 2002. Performance of a novel Viresolve NFR virus filter. Biotechnol Prog 18:782–795.

DiLeo AJ, Allegrezza AE, Builder SE. 1992. High resolution removal of virus from protein solutions using a membrane of unique structure. Nat Biotechnol 10:182–188.

DiLeo AJ, Vacante DA, Deane EF. 1993. Size exclusion removal of model mammalian viruses using a unique membrane system. Part II. Model qualification and process simulation. Biologicals 21:275–286.

Jackson NB, Bakhshayeshi M, Zydney AL, Mehta A, van Reis R, Kuriyel R. 2014. Internal virus polarization model for virus retention by the Ultipor® VF grade DV20 membrane. Biotechnol Prog 30:856–863.

Ireland T, Lutz H, Siwak M, Bolton G. 2004. Viral filtration of plasma-derived human IgG: A case study using Viresolve NFP. Biopharm Intl 17:38–44.

Lacasse D, Genest P, Pizzelli K, Greenhalgh P, Mullin L, Slocum A. 2013. Impact of process interruption on virus retention of small-virus filters. Bioprocess Intl 11:34–44.

Lute S. 2014. Mechanism of virus breakthrough during filter pausing. PDA/FDA Virus and TSE Safety Conference, Bethesda, MD.

Lute S, Bailey M, Combs J, Sukumar M, Brorson K. 2007. Phage passage after extended processing in small-virus-retentive filters. Biotechnol Appl Biochem 47:141–151.

Mosier-Boss PA, Lieberman SH, Andrews JM, Rohwer FL, Wegley LE, Breitbart M. 2003. Use of fluorescently labeled phage in the detection and identification of bacterial species. Appl Spec 57:1138–1144.

Woods MA, Zydney AL. 2014. Effects of a pressure release on virus retention with the Ultipor DV20 membrane. Biotechnol Bioeng 111:545–551.